This version of the article has been accepted for publication, after peer review and is subject to Springer Nature's AM terms of use, but is not the Version of Record and does not reflect post-acceptance improvements, or any corrections. The Version of Record is available online at: https://doi.org/10.1007/s00521-016-2778-6

To cite this article:

Gómez-Pérez, P., Caldeirinha, R.F.S., Fernandes, T.R. *et al.* Using artificial neural networks to scale and infer vegetation media phase functions. *Neural Comput & Applic* 29, 1563–1574 (2018). https://doi.org/10.1007/s00521-016-2778-6

Using Artificial Neural Networks to Scale and Infer Vegetation Media Phase Functions

Paula Gómez-Pérez [a,*], Rafael F. S. Caldeirinha [b],
Telmo Rui Fernandes [b], Iñigo Cuiñas [c]

[a] *Centro Universitario de la Defensa, Escuela Naval Militar (Defence University Centre, Spanish Naval Academy), Plaza de España, s/n, 36920 Marín (Spain).*

[b] *Instituto de Telecomunicações, Leiria, Portugal and Polytechnic Institute of Leiria, School of Technology and Management, Leiria (Portugal). He is also with the University of South Wales, Faculty of Engineering, Pontypridd (United Kingdom).*

[c] *Dept. de Teoría do Sinal e Comunicacións, Universidade de Vigo, Avda. Maxwell, s/n, 36310 Vigo (Spain).*

* Corresponding author: Paula Gómez-Pérez (paula@cud.uvigo.es)

Abstract

Accurate vegetation models usually rely on experimental data obtained by means of measurement campaigns. Nowadays, RET and dRET models provide a realistic characterization of vegetation volumes, including not only in-excess attenuation, but also scattering, diffraction and depolarization. Nevertheless, both approaches imply the characterization of the forest media by means of a range of parameters, and thus, the construction of a simple parameter extraction method based on propagation measurements is required. Moreover, when dealing with experimental data, two common problems must be usually overcome: the scaling of the vegetation mass parameters into different dimensions, and the scarce number of frequencies available within the experimental data set. This paper proposes the use of Artificial Neural Networks as accurate and reliable tools able to scale vegetation parameters for varying physical dimensions and to predict them for new frequencies. This proposal provides a RMS error lower than 1 dB when compared to unbiased measured data, leading to an accurate parameter extracting method, while being simple enough for not to increase the computational cost of the model.

Keywords - *Artificial neural networks; attenuation; prediction methods; propagation; telecommunications; vegetation.*

1. Introduction

Radio propagation prediction models represent essential tools for radio planners and service providers. They allow the optimization of the cell coverage and the minimization of unwanted phenomena like multipath or interferences. The initial radio propagation models for vegetation media provided estimates of the path loss for specific frequency bands [1]. However, such models were very simplistic in nature and based on a few vegetation and geometry related parameters. Several scientific works [2]-[4] suggested that vegetation environments will not only cause simple attenuation (due to absorption), but also more complex effects, such as scattering, diffraction and depolarization, and most of this mechanisms develop in random basis. Empirical radio propagation models are usually based on simple equations that do not take into account these complex effects [5], and, although they have demonstrated to provide low attenuation errors, they do not model the vegetation environment in its complete complexity.

The *Radiative Energy Transfer* (RET) based models [6] and, in particular, the *Discrete Radiative Energy Transfer* (dRET) [7] have successfully been used to simulate radiowave propagation, scattering and depolarization phenomena due to the presence of vegetation volumes in the radio path [8]-[10]. In particular, RET models the vegetation media as a random and statistically homogeneous medium, randomly filled with small discrete scatterers. Such scatterers might be characterized by a set of two parameters, $\square$ and $\square$, and one directional scattering profile usually referred as *"phase function"* or *"re-radiation function"* [11]. The phase function, *(θ)*, specifies the amount of radiation that is transferred from one direction to another due to the random (volume) scattering process, and it can be modelled by (1), where θ is the angle in degrees around the vegetation volume, $\square$ represents the width of the forward lobe and $\square$ is the ratio of the forward scattered to the total scatter power.

$$p(\theta) = \alpha \left(\frac{2}{\beta}\right)^2 e^{-\left(\frac{\theta}{\beta}\right)^2} + (1 - \alpha) \tag{1}$$

The phase function will consist of a narrow Gaussian forward lobe, superimposed to an isotropic background level, as shown in Figure 1(a). This figure shows an example of the measured re-radiation pattern of a *Ficus Benjamina* tree against its fitted phase function. Figure 1(b) and (c) represent the phase function for various values of the α and β parameters. Both parameters affect the shape of the phase function: whereas α controls the backscatter level, β

2

defines the half power beamwidth of the phase function forward lobe. Thus, having the phase function from the measured data, we can easily extract the parameters needed for RET model [11].
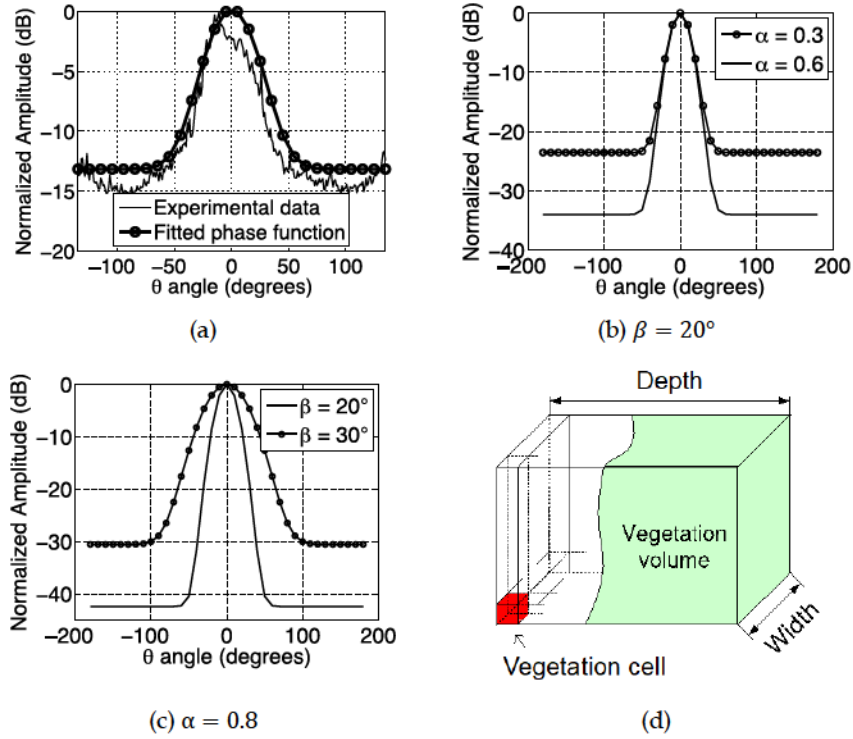

Figure 1. (a) Fitted phase function example for a *Ficus Benjamina* at 40 GHz (α=0.8 and β=20°); (b) and (c) Gaussian phase function for various α and β values; (d) Discretized vegetation volume for dRET modelling.

On the other hand, dRET deals with isolated volumes of vegetation, considering their influence on the propagation characteristics [12]. This approach is based on dividing the vegetation volume into several non-overlapping cells of normalized and unitary dimensions, as shown in Figure 1(d).

The dRET model relies on the same input parameters as the RET approach, involving the phase function. However, despite the efficiency of this method, there is an extremely difficult problem to overcome, that is, to scale the phase function for the unitary cells, which will probably have different dimensions from the measured vegetation cells. This process is so-called *parameter scaling*, and it is a recurrent problem when modelling vegetation masses or forested areas.

In [13] authors have demonstrated the ability of artificial neural networks (ANN) to retrieve discrete angle intervals of an incomplete re-radiation pattern. However, such model must be trained with a set of measurements in every desired frequency and/or dimensions, and thus, the problem of inferring a complete re-radiation function remains unsolved.

The aim of this paper is to propose the use of feedforward artificial neural networks (ANN) as reliable and accurate tools, which are perfectly capable to scale full vegetation phase functions to any new vegetation cell dimensions. This technique been selected among different methodologies such as polynomial regressions, because it has demonstrated its accuracy in [13] whereas it requires a lower number of coefficients and a smaller training set [14].

With a proper training process based on experimental data, an ANN will be able to accurately infer vegetation phase functions not only to scale into larger or smaller cells (*parameter scaling*), but also to infer and predict the phase function for new frequencies different than those measured (*frequency retrieval*). This methodology will be applied to one vegetation specie (*Ficus Benjamina*), given the popularity of this specie in radio propagation experiments ([4], [5], [7], [10]), but it could be extended to other species. A general model could also be obtained by adding different input features (such as the water content of the leaves, for example) but it is out of the scope of this paper.

Results obtained are presented as follows: Section 2 describes how the experimental data were obtained, whereas Section 3 details the neural network architecture and the design criteria followed. Section 4 provides a detailed exposure of the results obtained for different tests and the resulting model obtained, and finally, Section 5 outlines the conclusions drawn from the present work.

2. Obtaining the experimental data

The experimental data required to train the network are the outcome of a large measurement campaign. This section explains the measurement setup and procedure carried out for this experiment.

2.1. Measurement setup

A series of re-radiation functions measured around the vegetation element, from different illuminated vegetation volumes at 20, 40 and 62.4 GHz, allow the evaluation of parameter dependence on the size of the vegetation volume. The experiment involved the measurement of the phase function using the setup diagram presented in Figure 2 (a). Four *Ficus Benjamina* trees have been chosen as the vegetation specimens to perform these tests, with an average canopy diameter of 60 cm, and mean height of 1.5 meters.
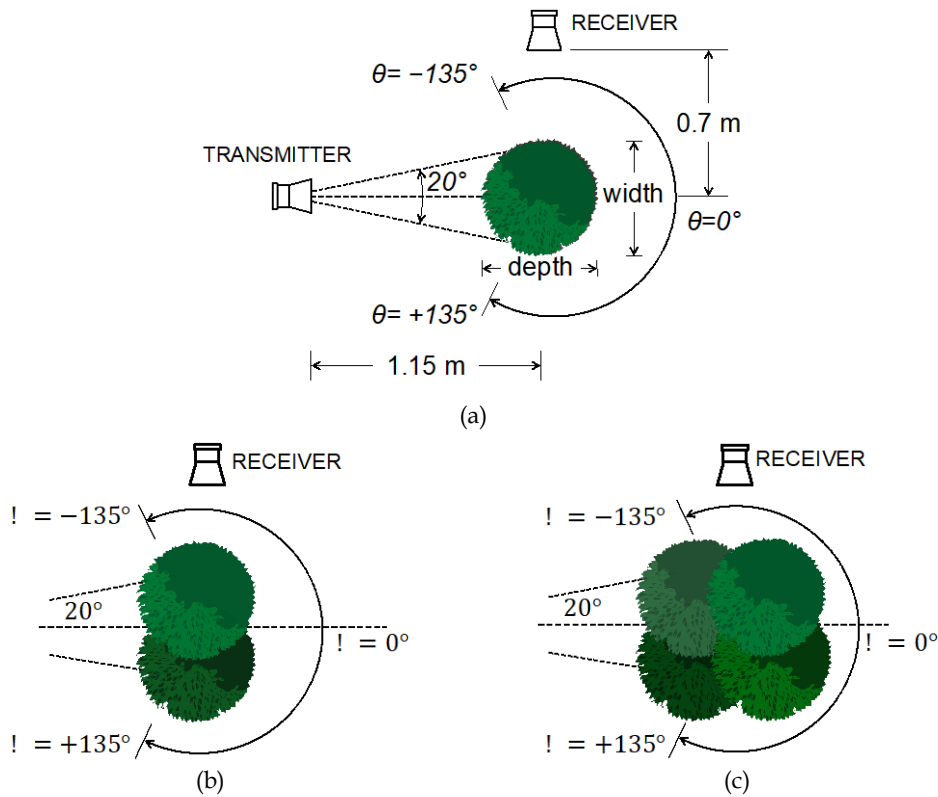

Figure 2. Measurement setup: (a) Indoor re-radiation function measurement setup (Top View general layout for 1-Tree); (b) Plant arrangement corresponding to 2-Tree volumes used in the parameter scaling measurement; and (c) Plant arrangement corresponding to 4-Tree volumes used in the parameter scaling measurement.

The measurements were performed inside an anechoic chamber by rotating the receiver along an arc around the tree within an angular range from -135° to 135°, with one degree of resolution. For each position of the receiver, the tree was rotated in a continuous movement 360° around its vertical axis [15]. This movement, which takes about 10 seconds, allows the receiver to acquire 1.000.000 samples at the maximum sampling rate of the data acquisition unit, yielding to 100.000 samples per second. The samples obtained during the tree rotation were averaged and the mean signal level was recorded, forming the tree re-radiation

function.

Measurements were carried out using 20 and 10 dBi standard horn antennas at the transmitter and the receiver, respectively. The distance between the transmitter antenna and the tree was chosen to be 1.15 m, ensuring that 2/3 of the 60 cm of the canopy diameter was illuminated within the antenna half power beamwidth [16]. This distance remained constant throughout all measurements performed.

Considering the obstacle as a sum of small discrete scatterers, the receiver antenna was in the intermediate Fresnel zone from the obstacle (in-between far-field and near-field distances), and, consequently, measurements were performed in a quasi-far field region from the scatterers. The transmitter antenna was located in its far-field range, which were 37.5, 21.3 and 68.3 cm for 20 40 and 62.4 GHz, respectively. However, the type of field analysed is irrelevant for the ANN, since it would infer the re-radiation pattern desired, as long as the training samples are correlated with those in the appropriate region.

2.2. Measurement procedure

The re-radiation measurements were performed in seven different cases corresponding to three different vegetation volume dimensions and one free space measurement, for the three frequencies under study, as follows:

- Free space measurement, with no vegetation volume between transmitter and receiver. This measurement will be used for normalization and reference purposes;

- Individual plants measured alone. The re-radiation function of each of the four *Ficus* plants was measured, leading to the scattering effect exhibited by each of the plant alone. Since the plants were similar but differ in their foliage density, re-radiation measurements of the four specimens have been averaged out to homogenize their phase function;

- Group of two plants placed side by side;

- Group of four plants forming a squared layout vegetation volume.

The distribution of the *Ficus* plants in the various vegetation volumes, used to determine the variation of the phase function parameters, is shown in Fig. 2 (b)

and (c). For the layouts consisting of two and four specimens, an overlapping on the plants of approximately 50% has been applied, in order to simulate the density of larger vegetation masses, instead of groups of individual plants.

Therefore, for each layout and frequency (20, 40 and 62.4 GHz), 271 averaged samples, in the angular range from -135° to 135° around the plant, will be collected.

3. Neural Network Architecture

This section provides an overview of the design criteria followed for the ANN used in this application.

3.1. Turning system variables into input and output features

Input variables (also called *input features*) to the ANN must capture most (if not all) of the relevant information related with the measurement system and the vegetation mass under study, i.e., the information susceptible to change from one sample to another. Therefore, parameters remaining constant for all the samples will be ignored, *e.g.* transmitter and receiver configurations, or canopy density and type of foliage, since all the vegetation specimens belong to the same specie and had similar characteristics.

In particular, since the aim of this research is to scale and infer vegetation phase function for different canopy sizes and frequencies, consideration should be given to input features such as the rotation angle around the tree ($\square$, in degrees), the frequency (in GHz), and the dimensions (depth and width) of the vegetation volume (in m).

Regarding the output variables, there will be only one output feature, which is the estimated power received at each angular position of the receiver around the vegetation volume (in dB), as shown in Fig. 2 (a). Since the output is an analogue variable, the resulting system may be classified as a *curve fitting* application. Hence, this will set most of the parameters of the neural network final design.

3.2. Signal pre-processing

Before feeding the neural network with the experimental data, a few pre-

processing must be done. First of all, to eliminate the dependence of the distance between transmitter and receiver, the power received has been normalized to the maximum power received in free space, without any tree in the line of sight.

Secondly, the samples have been randomized to ensure that the data inferred by the neural network is not just a simple interpolation of the data used in the training stage. Also, in each of the tests performed, a set of samples has been set aside from the training process, being left *out-of-bag* (OOB). Such sets will be used afterwards to validate the network generalization ability.

Finally, the input features have to be normalized, so that all of them will take values within the same range. If not applied, the system may "learn" that the features taking larger values (such as the frequency, in the range of GHz) are more important than the rest, and it might converge to an improper solution, or even diverge. This process is called *parameter scaling* and is defined by (2), where μ_i and σ_i are the mean value and the standard deviation of each input feature vector, x_i.

$$x_{i,normalized} = (x_i - \mu_i)/\sigma_i \qquad \text{for } i=1,...,4 \qquad (2)$$

Normalization parameters are calculated over the samples in the training set, and will be applied afterwards to all new samples entering the ANN.

3.3. Neural Network design

Artificial neural networks are computational systems designed to emulate a simplified behaviour of the brain by interconnecting basic elements, called neurons, arranged in consecutive layers. These neurons behave as mathematical blocks that combine linearly their input features and apply them an *activation function*.

An architecture of three layers has been chosen, as shown in Figure 3, which is the most typical layout for *curve fitting* applications [18]. Therefore, our proposal will be comprised of an input layer, receiving the input features; an output layer, generating the output signal; and an intermediate layer, called hidden layer, in charge of capturing the non-linear relationships between the input features, where:

l_1, l_2, l_3 refer to layer 1 (input layer), 2 (hidden layer) and 3 (output layer), respectively;

$n_{l_1}, n_{l_2}, n_{l_3}$ are the number of significant neurons in l_1, l_2 and l_3, respectively;

$a_i^{(k)}$ denotes the neuron i of the layer k, where $a_1^{(1)}$ and $a_1^{(2)}$ are the bias terms of the input and hidden layer, respectively;

$w_{i,j}^{(k)}$ is the weight that measures the importance of the interconnection between the neuron i of the layer $k+1$ and the neuron j of the layer k;

$W^{(1)}, W^{(2)}$ are the matrices containing the weight coefficients $w_{i,j}^{(1)}$ and $w_{1,j}^{(2)}$ that rule the interconnection between the neurons of the layer 1 to 2 and 2 to 3, respectively.

The size of the hidden layer and the activation function of its neurons will determine most of the ability of the network to extract the pattern of the phase function. For this application, we will have four significant neurons in the input layer (one per input feature) (i.e., $n_{l_1} = 4$) applying an identity function, and a single neuron in the output layer ($n_{l_3} = 1$) applying a linear function.
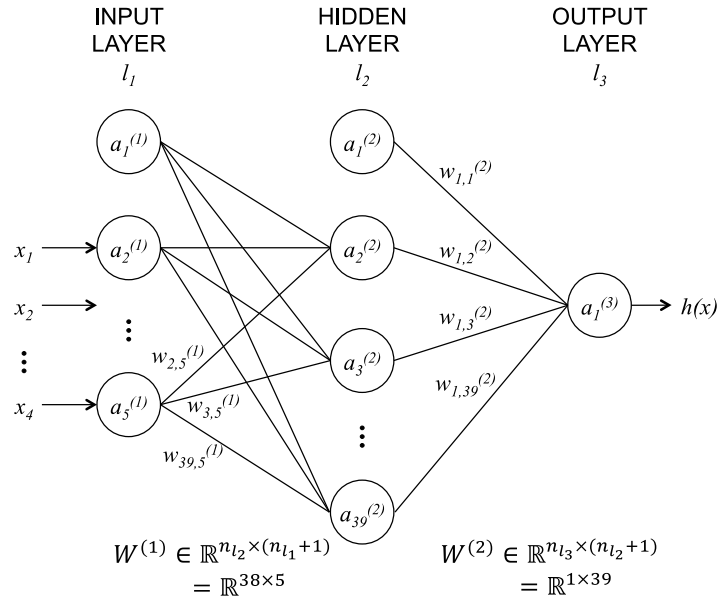

Figure 3. Artificial Neural Network architecture

The neurons in the hidden layer will have a *sigmoid* activation function, defined by (3), and will be the elements in charge of capturing the non-linearity relationships of our model.

$$g(\xi) = \frac{1}{1 + exp(-\xi)} \tag{3}$$

Once the basic design is established, the number of significant neurons of the hidden layer must be chosen, as well as a method to avoid the *over-learning* or *overfitting* of the network. The number of neurons has been chosen to be $n_{l_2} = 38$, because, for all the tests performed, it has demonstrated to be the lower dimension that minimizes the error obtained. Adding more neurons will not increase the "learning" ability of the network, but instead will increase computational costs.

Furthermore, neural networks are prone to learn "too well" the training data. This effect is called *overfitting* and is an undesirable effect, since the neural network will fail dramatically when trying to infer the output for new unseen samples. To avoid the overfitting, a regularization parameter might be introduced in the training stage, which is a constant value that maintains this effect under control. For this case, a regularization parameter of 0.003 has been proved to be good enough for all tests performed.

Based on this design, the outcome of the ANN will be ruled by equations (4) to (8), where $a_1{}^{(1)}$ and $a_1{}^{(2)}$ in (4) and (6) represent the *bias* terms in the input and hidden layer, respectively, and $a_i{}^{(1)}$, $a_i{}^{(2)}$ and $a_i{}^{(3)}$ represent the output of the input, hidden and output layer, respectively. *Bias* terms are necessary for the ANN model, but they are not acknowledged as significant neurons, since their output is constant for all the samples.

$$a_1^{(1)} = 1 \tag{4}$$

$$a_i^{(1)} = x_{i-1} \quad \text{for } i=2,...,5 \tag{5}$$

$$a_1^{(2)} = 1 \tag{6}$$

$$a_i^{(2)} = \frac{1}{1+exp\left(-\sum_{j=1}^{n_{l_1}+1} w_{i,j}^{(1)} \cdot a_j^{(1)}\right)} \quad \text{for } i=2,...,39 \tag{7}$$

$$a_1^{(3)} = \sum_{j=1}^{n_{l_2}+1} w_{1,j}^{(2)} \cdot a_j^{(2)} = h(x) \tag{8}$$

Training an ANN will consist in obtaining the weights $w_{i,j}{}^{(1)}$ and $w_{1,j}{}^{(2)}$ that

govern the linear combinations of the neurons in (7) and (8). This parameter extraction will be carried out iteratively using the backpropagation algorithm along with global descent to avoid local minima [18] [19], to obtain the matrices $W^{(1)}$ and $W^{(2)}$ that contain the desired coefficients.

Matrices $W^{(1)}$ and $W^{(2)}$ were initialized to small random numbers within the range $[-\epsilon, +\epsilon]$ (*i.e.*, $-\epsilon \leq w_{i,j}^{(k)} \leq \epsilon$), being ϵ a small value between $[0,1]$ ($\epsilon = 0.15$ for this case) [18]. This random initialization might lead to different outcomes from one training to another. Therefore, the robustness of the ANN was tested beforehand, to check the independency on the initial values. To do so, several different trainings were carried out, and results of the inferred attenuations were compared for each case. It was demonstrated that, due to the robustness of the ANN architecture chosen and the large training set size, all ANNs converged into similar outcomes, where the differences in the attenuation inferred from one network to another were negligible (lower than 10^{-2}, in terms of RMS Error). Hence, the independency on the initialization values is ensured.

Despite the relatively small complexity of the architecture selected, it will suffice to obtain an efficient and accurate model, able to infer and scale vegetation re-radiation patterns with an RMS error lower than 1 dB for all the cases under study, as section 4 will show.

4. Experimental results and analysis

This section details the tests carried out to demonstrate the ability of the ANN to scale the phase function of a vegetation mass, and to infer the phase function for new frequencies, unseen before by the ANN.

4.1. Using neural networks to scale vegetation phase function

Three different tests have been carried out in order to demonstrate the generalization ability of the ANN to scale the phase function of a vegetation mass. Firstly, we will show the ability of the network to scale the phase function of a vegetation mass for an unknown size, which is in between known dimensions. Therefore, the system will be trained with the samples corresponding to the dimensions of a single tree and the formation of four trees, and we will test the network RMS error when inferring the power received for the case of two trees. For this first experiment, the samples for the formation of

two trees have been completely set aside from the training set, remaining OOB, whereas the rest of the samples have been used to train the neural network. Table 1 (test 1 to 3) resumes the samples used in each of the test performed.

Table 1

Test performed to check the Scaling Ability (Test 1 to 3) and the Frequency Retrieval Ability (Test 4 to 6) of the ANN, and Training and OOB samples used in each test

Test Number	Layout	Frequency		
		20 GHz	40 GHz	62.4 GHz
Test 1 (obtaining 2-Trees)	1-Tree	Train	Train	Train
	2-Trees	**OOB**	**OOB**	**OOB**
	4-Trees	Train	Train	Train
Test 2 (obtaining 4-Trees)	1-Tree	Train	Train	Train
	2-Trees	Train	Train	Train
	4-Trees	**OOB**	**OOB**	**OOB**
Test 3 (obtaining 1-Tree)	**1-Tree**	**OOB**	**OOB**	**OOB**
	2-Trees	Train	Train	Train
	4-Trees	Train	Train	Train
Test 4 (obtaining 40 GHz)	1-Tree	Train	**OOB**	Train
	2-Trees	Train	**OOB**	Train
	4-Trees	Train	**OOB**	Train
Test 5 (obtaining 20 GHz)	1-Tree	**OOB**	Train	Train
	2-Trees	**OOB**	Train	Train
	4-Trees	**OOB**	Train	Train
Test 6 (obtaining 62.4 GHz)	1-Tree	Train	Train	**OOB**
	2-Trees	Train	Train	**OOB**
	4-Trees	Train	Train	**OOB**

Fig. 4 (a), (b) and (c) show the results of the interpolation performed by the neural network, demonstrating the capacity of the network to infer properly the phase function for intermediate dimensions. When the signal becomes noisier, the prediction slightly reduces its accuracy, as can be seen in the Fig. 4 (a) and (b). Since the neural network extracts the envelope of the signal, it does not follow fast changes, so smooth measurements will provide better accuracies in the prediction of the neural network, as can be appreciated in Fig. 4 (d) or (f), where the experimental data show less variance.
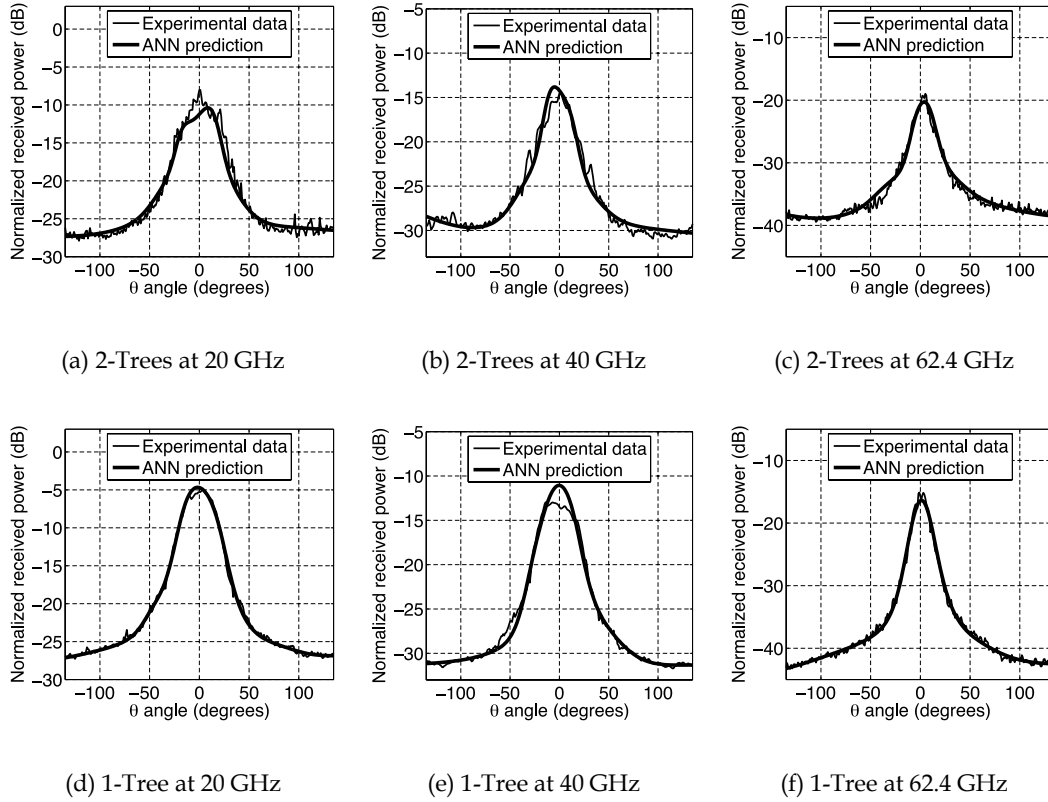
Figure 4. Comparison of the curves derived from experimental data vs. the inferred phase function by the ANN when testing the scaling ability of the ANN into different dimensions.
Test performed for 2-Trees layout at (a) 20 GHz, (b) 40 GHz and (c) 62.4 GHz; and for 1-Tree layout at (d) 20 GHz, (e) 40 GHz and (f) 62.4 GHz.

However, when dealing with vegetation measurements, and specially with RET and dRET models, the most common scenarios might involve having the power received from very large forested areas and need to scale them into unitary elements; or having small vegetation specimens, usually measured into an anechoic chamber, and need to scale their phase function into larger vegetation volumes. Those two cases will consist in scaling from 4-trees layout to 1-tree layout, and from 1-tree to 4-trees layout, respectively. These are referred to as extrapolation cases for the neural network. For both cases, each of the samples to be inferred are left out of the training set, compounding the OOB set, to be able to test, afterwards, the ability of generalization of the neural network. Table 1 (test 2 and 3) specifies the samples used in each case.

Fig. 4 (d), (e) and (f) show the results of the extrapolating case when scaling into unitary dimensions. Again, the ANN is able to follow the original data, although

14

it has not been trained specifically with these dimensions. For this case, the prediction of the neural network seems to be more accurate than the rest of the tests performed. This is due to the lower variance of the input signal, because it is the result of averaging the power received by the four *Ficus* specimens. Since the input signal is smoother, the prediction of the neural network will obtain a lower error when compared with the averaged experimental data. Therefore, it could be stated that, for dense vegetation species, such as conifers, the neural network will scale the phase functions even better than in this case, since the power received by denser species usually have more stable (and therefore, smoother) phase functions.

Table 2 shows the RMS error obtained by the ANN when comparing the inferred response of the vegetation mass with the measured phase function. The obtained error, observed to be lower than 1 dB for all tests, demonstrates the capability of the neural networks to scale accurately the phase function of vegetation volumes.

Table 2
RMS Error obtained by the ANN when fitting the Phase Function

	RMS Error (dB)	
Phase Function Scaling	Test 1 (scaling to unitary cell)	0.88
	Test 2 (scaling to double cell)	0.74
	Test 3 (scaling to quadruple cell)	0.58
Phase Function Frequency Retrieval	Test 4 (inferring 40 GHz)	0.73
	Test 5 (inferring 20 GHz)	0.70
	Test 6 (inferring 62.4 GHz)	0.68

4.2. Using neural networks for frequency retrieval

We will now show that neural networks are also powerful tools that can retrieve and infer the phase function of vegetation masses at any desired frequency. To this extent, the results of three different tests will be presented: the first one will obtain the phase function for the interpolated frequency of 40 GHz. The second and third cases correspond to the extrapolation cases, where the network has to infer completely new frequencies. In every test carried out, the samples corresponding to each case have been set aside from the training set. Table 1 (test 4 to 6) resumes the samples used in each of the test performed.

Fig. 5 (a), (b) and (c) show the results of the inferred intermediate frequency of 40 GHz after training the neural network with the samples of 20 and 62.4 GHz.

Again, the curve provided by the ANN is able to infer the data with a very low error, which increases with the variance of the experimental data, as can be seen in the Fig. 5 (b) and (c) for the layouts of 2- and 4-trees, respectively. Fig. 5 (d) to (f) show the prediction of the phase function at 62.4 GHz (extrapolated frequency), for a network that has only been trained with the frequencies of 20 and 40 GHz.

| (a) 1-Tree at 40 GHz | (a) 1-Tree at 40 GHz | (a) 1-Tree at 40 GHz |

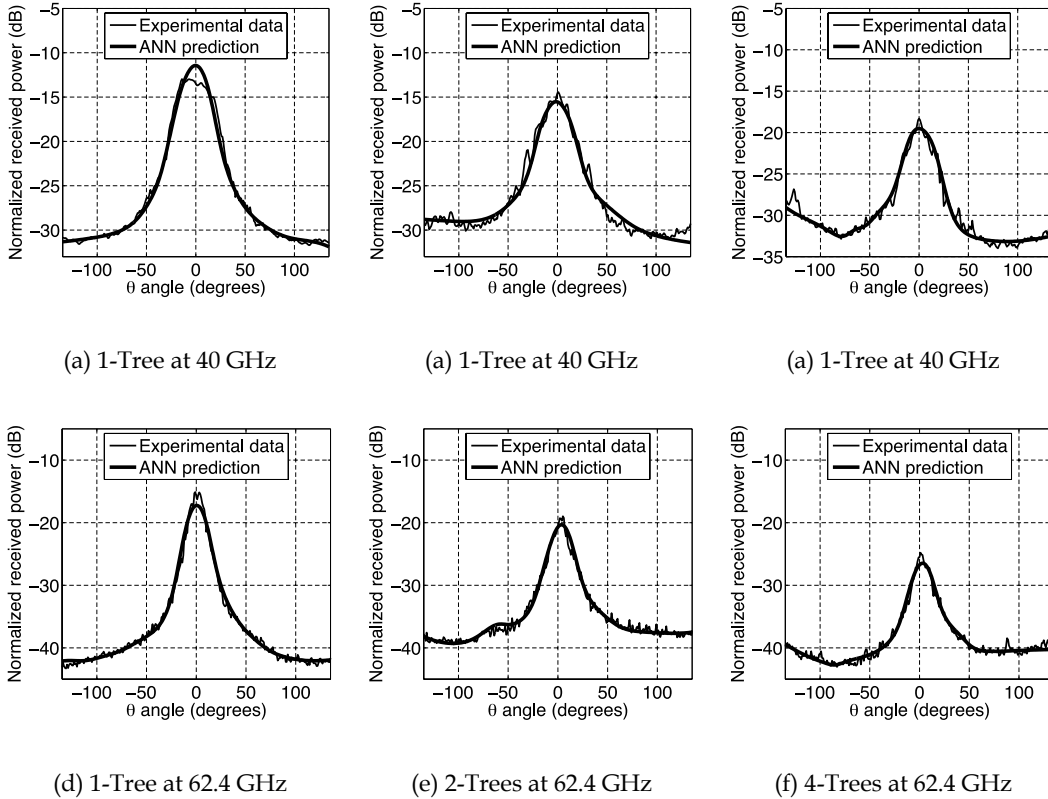| (d) 1-Tree at 62.4 GHz | (e) 2-Trees at 62.4 GHz | (f) 4-Trees at 62.4 GHz |

Figure 5. Comparison of the curves derived from experimental data vs. the inferred phase function by the ANN when testing the ability to retrieve different frequencies.
Test performed at 40 GHz for (a) 1-Tree layout, (b) 2-Trees layout and (c) 4-Trees layout; and at 62.4 GHz for (d) 1-Tree layout, (e) 2-Trees layout and (f) 4-Trees layout.

The extrapolation cases seem to work better than the interpolation one, mostly because the experimental data conform a smoother function than in the interpolate case. As commented before, the neural network will infer more accurately such cases, since it works better for signals with low variance.

The small error obtained by the neural network, which is capable of predicting accurately the phase function for new frequencies, demonstrate the ability of the neural network to infer the phase function at frequencies unseen in the training

16

stage. Again, Table 2 shows the RMS errors of the neural network prediction for these three tests, which is lower than 1 dB for the entire experiments performed, validating the proposal of this paper.

4.3. Comparison with current methodology

Current methodology to obtain vegetation phase functions consists in fitting available measurements to the Gaussian-shape defined by (1) by means of brute-force, i.e., testing different values for α and β until the best fit is found. To generalize into new dimensions or frequencies, the common procedure consists in interpolate or extrapolate α and β, using the parameters derived from the available measurements. Results obtained by this interpolation method will fail to generalize into new scenarios, because parameters α and β do not follow a linear relationship with frequency or vegetation dimensions.

This approach has an additional major problem that cannot be overcome, which is that it provides normalized amplitudes to 0 dB, and thus, the real power received is unknown for new unmeasured data. On the contrary, neural networks can scale accurately both the shape of the phase function and the power re-radiated by the vegetation mass, providing an idea of the in-excess attenuation introduced by the vegetation element in the line of sight.

To validate the proposal of his paper, Test 1 has been performed using both methodologies, to obtain the phase function of a 2-Trees layout at 40 GHz based on the measurements for 1-Tree and 4-Trees at that frequency. For the interpolation method, we fit by force-brute two phase functions for the samples available in the training set, resulting in *α=0.7, β=15º* for 1-Tree samples and *α=0.7, β=25º* for 4-Trees samples. These values are interpolated to obtain the scaled α and β at the intermediate dimensions of 2-Trees, resulting in *α=0.7, β=20º*. Secondly, we will infer the phase function provided by the ANN, and use the result to fit the best phase function possible by means of (1) *(α=0.7, β=29º)*.

Fig. 6 shows the results obtained, where all plots have been normalized to 0 dB, for the sake of the comparison. We can see that the phase function inferred by the ANN follows closely the best fit plot, since they practically overlap, whereas interpolated fit provides accuracy only in a short angular interval ranging from -25° to 25°. For this particular case, RMS errors obtained are 0.78 dB for the ANN approach, 1.8 dB for the ANN fitted phase function, and 4.5 dB for the interpolated method.
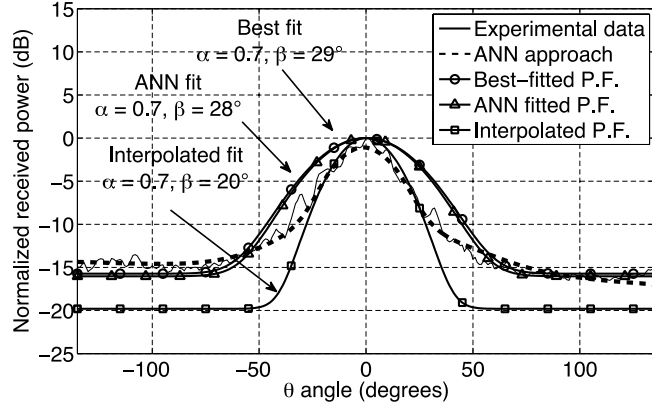
Figure 6. Comparison between the ANN approach and the interpolated phase function (P.F.) for Test 1, 2-Trees configuration.

If normalization to 0 dB is not performed, the error provided by the interpolated method will rise to 7.8 dB, since the plot obtained will be shifted upwards relatively to original measurements. On the contrary, the RMS error of the ANN will remain constant, since it is able to infer closely the power received for this unknown scenario.

Therefore, results obtained validate the proposal of this paper.

5. ANN model obtained

Tests 1 to 6 have demonstrated the ability of neural networks to scale and infer accurately re-radiation functions into new vegetation dimensions and frequencies. To obtain a general model, we performed a new test, where all samples have been shuffled and divided in three sets: a training set, a cross-validation set, and a test set (which will be the OOB samples), containing the 60%, 20% and 20% of the measurements, respectively.

The network has been trained with the data of the training set, applying regularization and early stop to avoid overfitting, using the cross-validation set [18]. We validated the model obtained over the test set, and calculated the RMS errors in the three sets, being: 0.16 dB for the training set, 0.25 for the cross-validation set and 0.31 for the test set. Final RMS error is lower than Tests 1 to 6 because now the ANN has more samples to be trained on, and thus, it will fit better the data, reaching better accuracies.

Table 3 in the Appendix contains the normalization values extracted from the training set, that will have to be applied to any new input data entering the ANN, whereas Table 4 and 5 show the coefficient matrices $W^{(1)}$ and $W^{(2)}$ for the proposed model, containing the parameters $w_{i,j}^{(1)}$ and $w_{1,j}^{(2)}$.

The algorithm to calculate the outcome of the neural network might be as follows:

(i) Normalize the new input features using (2) and corresponding values in Table 3.

(ii) Calculate the input features vector, $a^{(1)}$ as (6) indicates, being x_i the new normalized data for the *i-th* variable;

(iii) Obtain $a^{(2)}$ applying (7) and coefficients $W^{(1)}$ in Table 4;

(iv) Calculate the inferred attenuation, $h(x)=a^{(3)}$, following (8) and coefficients $W^{(2)}$ in Table 5.

6. Conclusions

In this paper we have demonstrated the capability of artificial neural networks to be used as powerful and simple tools to obtain the parameters needed to characterize vegetation masses. In particular, we have shown that neural networks are able to properly scale the phase function of vegetation masses into larger or shorter dimensions, and to retrieve the phase function data for new frequencies other than those used in the data gathering.

Several neural networks have been trained, maintaining the design parameters but varying the training data to perform the different tests. An RMS error below 1 dB was obtained for every of the cases proposed, confirming the generalization capability of these machine-learning systems.

An accurate final ANN has been trained, and the resulting coefficient matrices and methodology to be applied have been shown. This model has a high accuracy with a RMS error lower than 0.4 dB, which validates the proposal of this paper. These experiments aimed a single vegetation specie (*Ficus Benjamina*), since the goal was to test the ability of the network to properly scale vegetation

parameters and infer new frequencies. An interesting future line might be measuring the re-radiation function for several other species and specimens, and including this information in the form of new input features to the system, to increase the generalization ability of the system.

The methodology proposed in this paper can be extended to any vegetation volume that can be considered as a whole, which includes isolated specimens, but also tree formations, such as chains of trees. For example, in a chain or clump of trees, if the individual elements are close enough to each other, the illuminated area by the transmitter could be modelled as a 4-Trees or n-Trees case, and the ANN will still provide results more accurate than current methodology.

As a general conclusion, artificial neural networks have demonstrated to be a good method to scale vegetation parameters, and to infer them for new frequencies. It is envisaged that the outcomes of this work can be used as input parameter optimization and refinement to the current ITU-R P.833-8 generic model for attenuation in vegetation media.

Appendix

Table 3

Values for μ and σ to normalize new samples

	θ (°) x_1	Frequency (GHz) x_2	Depth (m) x_3	Width (m) x_4
μ	0.6263	39.6617	1.1686	1.3321
σ	1.3321	16.2572	16.2572	16.2572

Table 4
W⁽¹⁾ matrix of weights of the ANN

Table 4

$W^{(1)}$ matrix of weights of the ANN

	$w_{i,1}$	$w_{i,2}$	$w_{i,3}$	$w_{i,4}$	$w_{i,5}$
$w_{1,j}$	-1.8478	0.0947	0.9024	-0.5655	-0.3132
$w_{2,j}$	-1.8733	0.1898	1.0103	-0.6091	-1.2952
$w_{3,j}$	-1.6112	3.1081	2.6996	0.4106	-2.6029
$w_{4,j}$	-7.162	-2.8454	3.3663	-0.7809	0.7758
$w_{5,j}$	-1.5021	0.0469	0.7088	-0.4391	-0.5221
$w_{6,j}$	-4.8409	-0.8674	1.4015	-0.6665	-0.438
$w_{7,j}$	-2.3195	0.1551	2.71	1.2852	-0.2139
$w_{8,j}$	-1.5135	0.0354	0.8036	-0.5799	-0.2492
$w_{9,j}$	-1.1443	1.3026	-0.527	2.1611	0.0385
$w_{10,j}$	-1.6737	0.0264	1.2083	0.0171	0.102
$w_{11,j}$	-1.8477	0.0217	1.7081	0.3526	-0.6291
$w_{12,j}$	-1.3825	-0.4304	3.1013	-0.1028	0.5196
$w_{13,j}$	-1.5594	0.0187	0.6324	-0.5308	-0.2404
$w_{14,j}$	-3.7613	0.0005	2.0507	-0.1332	-1.1345
$w_{15,j}$	-1.8223	0.085	2.2836	0.7597	-0.7146
$w_{16,j}$	-3.0081	0.1551	1.4317	-0.2693	-0.3945
$w_{17,j}$	-0.6906	-1.3819	0.1423	-2.3585	1.7231
$w_{18,j}$	-3.3939	4.373	-0.9953	-2.6896	-0.3391
$w_{19,j}$	-2.8051	-11.1815	1.1949	0.1703	0.3301
$w_{20,j}$	-0.8255	-2.2516	0.9032	0.6017	-0.01
$w_{21,j}$	-1.3261	0.5265	1.5225	-0.3657	-2.0195
$w_{22,j}$	-3.0728	10.292	0.5168	0.025	-0.3347
$w_{23,j}$	-2.6877	0.211	1.4846	-0.5832	-0.5267
$w_{24,j}$	-2.2365	-12.5282	0.7055	-0.5103	0.9158
$w_{25,j}$	-3.2388	-6.6478	0.088	-1.401	-0.5677
$w_{26,j}$	-4.6984	-12.8899	2.8055	0.2935	0.1103
$w_{27,j}$	-0.0041	6.1472	2.0865	2.0513	1.9028
$w_{28,j}$	-4.1279	-6.0578	0.985	0.4499	0.5703
$w_{29,j}$	-2.1622	-9.1553	0.6049	0.1725	0.2512
$w_{30,j}$	-0.6048	2.5093	5.4355	0.529	4.9494
$w_{31,j}$	-2.4706	-0.0832	1.2488	0.1705	-0.6996
$w_{32,j}$	-0.9455	8.8424	-0.3204	0.29	0.971
$w_{33,j}$	-1.556	0.0325	0.644	-0.6418	-0.1754
$w_{34,j}$	-3.2903	-7.8612	1.2789	0.2739	0.2491
$w_{35,j}$	-1.2034	-0.3506	2.9507	0.1598	0.0216
$w_{36,j}$	0.4578	6.5461	-0.8967	6.5929	0.0243
$w_{37,j}$	3.5713	12.2529	-3.7238	0.0754	0.1457
$w_{38,j}$	-2.9835	0.7601	3.0806	2.0861	0.4553

Table 5

$W^{(2)}$ matrix of weights of the ANN

$w_{1,1}$ 5,6387	$w_{1,11}$ -0.1010	$w_{1,21}$ 2.1959	$w_{1,31}$ -3.3950
$w_{1,2}$ -0.9965	$w_{1,12}$ -0.9952	$w_{1,22}$ -1.1564	$w_{1,32}$ -1.3790
$w_{1,3}$ -1.4564	$w_{1,13}$ -1.6672	$w_{1,23}$ -10.2345	$w_{1,33}$ -6.5321
$w_{1,4}$ -2.0524	$w_{1,14}$ -0.3659	$w_{1,24}$ -1.8100	$w_{1,34}$ -0.4967
$w_{1,5}$ -4.8272	$w_{1,15}$ -2.4714	$w_{1,25}$ -5.7693	$w_{1,35}$ -2.9474
$w_{1,6}$ -0.3706	$w_{1,16}$ -1.4635	$w_{1,26}$ -3.0853	$w_{1,36}$ -1.5191
$w_{1,7}$ -2.3602	$w_{1,17}$ -1.7340	$w_{1,27}$ -8.2578	$w_{1,37}$ -5.7866
$w_{1,8}$ -1.8779	$w_{1,18}$ -2.074	$w_{1,28}$ -2.6329	$w_{1,38}$ -9.6771
$w_{1,9}$ -0.5642	$w_{1,19}$ 4.8584	$w_{1,29}$ -3.8480	$w_{1,39}$ -2.5149
$w_{1,10}$ 3.1991	$w_{1,20}$ -4.6325	$w_{1,30}$ -3.1089	

References

[1] Radiocommunication Assembly, Recommendation ITU-R P.833-8, Attenuation in Vegetation, ITU-R, 2013.

[2] F. Wang, and K. Sarabandi, "A Physics-Based Statistical Model for Wave Propagation through Foliage," *IEEE Trans. Antennas Propag.*, vol. 55, pp. 958–968, Mar. 2007.

[3] F. Mani, and C. Oestges, "A Ray Based Method to Evaluate Scattering byVegetation Elements," *IEEE Trans. Antennas Propag.*, vol. 60, pp. 4006–4009, Aug. 2012.

[4] A. V. Alejos, M.G. Sánchez, I. Cuiñas, and P. Gómez, "Depolarization effect by wind incidence on vegetation at 40 GHz", *2nd European Conf. on Ant. and Prop. (EuCAP 2007)*, 2007 pp. 1–6.

[5] P. Gómez, I. Cuinas, A. Alejos, M.G. Sánchez, and J.A. Gay-Fernández, "Analysis of the performance of vegetation barriers to reduce electromagnetic pollution," *IET Microw. Antennas Propag.*, vol. 5, no. 6, pp. 651–663, Apr. 2011.

[6] G. Picard, T. Toan, S. Quegan, Y. Caraglio, and T. Castel, "Radiative transfer modeling of cross-polarized backscatter from a pine forest using the discrete ordinate and eigenvalue method," *IEEE Trans. Geosci. Remote Sens.*, vol. 42, no. 8, pp. 1720–1730, Aug. 2004.

[7] T.R. Fernandes, R.F. S. Caldeirinha, M. AL-Nuaimi, and J. Richter; "A discrete RET model for millimeter-wave propagation in isolated tree formations," *IEICE Trans. on Communications*, vol. E88-B, no. 6, pp. 2411–2418, Jun. 2005.

[8] R. B. L. Stephens, and M. O. Al-Nuaimi, "Measurement and prediction model optimization for signal attenuation in vegetation media at centimeter wave frequencies," *IEE Proc. Microw. Antennas Propag.*, vol. 145, pp. 201–206, Jun. 1998.

[9] J. Richer, R. Caldeirinha, and M. Al-Nuaimi, "A generic narrowband model for radiowave propagation through vegetation", *Proc. IEEE 61st Veh. Technol. Conf. (VTC Spring)*, 2005, vol. 1, pp. 39–43.

[10] T. Fernandes, R. F. S. Caldeirinha, M. O. Al-Nuaimi, and J. Richter, "Radiative Energy Transfer based model for radiowave propagation in inhomogeneous forests", *Proc. of the 64th IEEE Vehicular Tech. Conf. (VTC 2006-Fall)*, vol. 1, Montreal, Quebec Canada, 2006.

[11] A. Ishimaru, *Wave propagation and scattering in random media*, IEEE Press, 1997, pp. 5–93.

[12] J. Richter, M.O. Al-Nuaimi, R. Caldeirinha, and N. Savage, "RET input parameter estimation for a generic model of propagation through vegetation using excess attenuation and phase function measurements", *12th Int. Conf. Antennas Prop., 2003. (ICAP 2003)*, vol. 2, no. 491, April 2003 pp. 836 – 839.

[13] P. Gómez-Pérez, R.F.S. Caldeirinha, T.R. Fernandes, I. Cuiñas, "Retrieving vegetation reradiation patterns by means of artificial neural networks", *IEEE Antenn. Wirel. Pr.*, vol. 15, issue 1, October 2015.

[14] P. Gómez-Pérez, M. Crego-García, I. Cuiñas, "Modeling vegetation attenuation patterns: A comparison between polynomial regressions and artificial neural networks", *2016 IEEE Int. Symp. on Antennas and Prop. (2016 AP-S/URSI)*, June 26 – July 1, Fajardo Puerto Rico, 2016.

[15] D. Didascalou, M. Younis, and W. Wiesbeck, "Millimeter-wave scattering and penetration in isolated vegetation structures," *IEEE Trans. Geosci. Remote Sens.*, vol. 38, pp. 2106–2113, Sept. 2000.

[16] F.T. Ulaby, T.E. Van Deventer, J.R. East, T.F. Haddock, and M.E. Coluzzi, "Millimeter-wave bistatic scattering from ground and vegetation targets," *IEEE Trans. on Geosci. Remote Sens.*, vol. 26, no. 3, pp. 229–243, 1988.

[17] C.A. Balanis, *Antenna theory: analysis and design*. John Wiley & Sons, Ltd. (2nd Edition), USA, 2005, pp. 60–63.

[18] C.M. Bishop, *Neural Networks for Pattern Recognition*, Oxford University Press, USA, 1995, pp. 77–100.

[19] V. Kecman, *Learning and Soft Computing, Support Vector Machines, Neural Networks, and Fuzzy Logic Models,* The MIT Press, Cambridge, 2001.